Minimizing the torsional response of asymmetric wall-type systems considering soil-structure interaction

H. Shakib[1,*], G.R. Atefatdoost[1]

Abstract

An approach was formulated for the nonlinear analysis of three-dimensional dynamic soil-structure interaction (SSI) of asymmetric buildings in time domainin order to evaluate the seismic response behavior of torsionally coupled wall-type buildings. The asymmetric building was idealized as a single-storey three-dimensional system resting on different soil conditions. The soil beneath the superstructure was modeled as nonlinear solid element. As the stiffness of the reinforced concrete flexural wall is a strength dependent parameter, a method for strength distribution among the lateral forceresisting elementswas considered. The response of soil-structure interaction of the system under the lateral component of El Centro 1940 earthquake record was evaluated and the effect of base flexibility on the response behavior of the system was verified. The results indicated that the base flexibility decreased the torsional response of asymmetric building so that this effect for soft soil was maximum. Onthe other hand, thetorsional effects can be minimized by using a strength distribution,when the centre of both strength CV and rigidity CR is located on the opposite side of the centre of mass CM, and SSI has no effect on this criterion.

Keywords: Torsional response, Asymmetric wall-type buildings, Nonlinear dynamic soil-structure interaction, Strength distribution, Stiffness eccentricity, Strength eccentricity.

1. Introduction

Non-uniform distribution of mass, stiffness and strength in asymmetric buildings cause the buildings to experience torsional moments and rotational deformation about vertical axes.Consequently, asymmetric buildings are more vulnerable to earthquake hazards compared to the buildings with symmetric configuration [1]. The recognition of this sensitivity has led the researchers (like Kan and Chopra 1977) to concentrate their studies on the earthquake characteristics, evaluation of structural parameters and validity of system models [2, 3 and 4]. In the seismic design of structures, one task after establishment of the base shear is the distribution of design strength among the lateral force resisting elements (LFRE). In order to mitigate the effect of torsion during the earthquakes, most seismic codes of the world provide design guidelines for strength distribution based on the traditional perception that element stiffness and strength are independent parameters.

It is known that, for an important class of widely used structural elements such as reinforced concrete flexural walls, stiffness is a strength dependent parameter.

This implies that the lateral stiffness distribution in a wall-type system cannot be defined prior to the assignment of the elements' strength. Therefore, both stiffness and strength eccentricity are important parameters affecting the seismic response of asymmetric wall-type systems [5].

In traditional approach, it is assumed that stiffness of an LFRE can be estimated independent of its strength. As a result of this assumption, the stiffness distribution is considered as known prior to the allocation of strength. Since the stiffness distribution is as known, the centre of rigidity (CR) and the stiffness eccentricity, e_R,which is defined as the distance between the centre of mass (CM) and (CR), can be readily determined. For this reason, e_R has become the parameter commonly used in the torsional provisions. Although the studies before 1997 mainly used this approach but it is only proper for LFREs,in which the stiffness and strength are independent. Another approach has been suggested for stiffness-strength dependent LFREsby Paulay (1997) based on the plastic mechanism analysis,in which he considered the behavior of single story building for this type of element, and concluded that the current lateral strength distribution of seismic code is inappropriate [6]. Tso and Myslima. F (2003) proved that the yield displacement distribution-based strength assignment between the resisting elements does not require the knowledge of stiffness distribution prior to strength assignment. They studied the problem of resisting elements having strength-dependent stiffness by

* Corresponding author: shakib@mail.modares.ac.ir
1 School of Civil Engineering, TarbiatModares University, Tehran, Iran

means of a one-storey model under one-directional excitations, and concluded that a desirable distribution of mass, stiffness and strength to reduce torsional response locates the CR and CVon the opposite sides of CM, a condition referred to as 'balanced CV–CR location' [7, 8]. Strictly correlated with these studies is the paper by Aziminejad and Moghadam (2006) who investigated the nonlinear behavior of code designed irregular single-storey structures in order to optimize configuration of mass, stiffness and strength centers with respect to different levels of plastic excursions in the framework of performance-based seismic design. It turned out that the balanced location, proposed by Tso and Myslimaj, optimized the system response at the life safety performance level (i.e., when the system is subjected to large inelasticity), whereas this was not the case in the elastic range of behavior. Furthermore, it was found that the best configuration varies not only with the assumed performance level, but also with the selected response parameters or damage indices. In this respect, the balanced location did notattain the minor ductility demands to the resisting elements of edges [9]. Shakib and Ghasemi (2007) considered different criteria for minimizing the torsional response of asymmetric structures under near-fault and far-fault excitations. They concluded that in near-fault ground motions, the minimum rotational response, considering the actual behavior method, could be achieved when stiffness and strength centers are located on the opposite sides of the mass center. By increasing pulse period of fault-normal component, displacement ductility demand increases as well. Rotational responses would be divided into three regions, which are related to $\frac{T}{T_P}$ ratio. Within $\frac{T}{T_P} \geq .50$, minimum and maximum rotational responses would occur. However, variation of rotational demand would be minimized for the range of $\frac{T}{T_P} = 1$. Within $\frac{T}{T_P} = 1$, the rotational demand increases with increasing of the stiffness eccentricity [10].

Aziminejad and Moghadam (2009)considered different strength distributions in multi-story asymmetric building and studied the effect of different distribution strategies on building response in the performance-based design approach. They concluded that the model with smaller strength eccentricity performs better. However, in general, optimum strength eccentricity is a function of the selected damage index [11].

Because of deformations within the soil immediately beneath a structure, the motion of the base of a building may differ from the motion of the ground at some distance away. Such a difference is indicative of soil-structure interaction. Interaction effects refer to the fact that the dynamic response of a structure built on a site depends not only on the characteristics of the free-field ground motion but also on the inter-relationship of dynamic structural properties and those of the underlying soil deposits [12]. Previous researches have shown that, for a specific structure, the responses during an earthquake may be totally different when the structure is founded on deformable soil compared to a structure with fixed base.

This difference is due to the fact that SSI may increase the natural periods of the systems, change the system damping due to wave radiationor modify the effective seismic excitation.The importance of soil-structure interaction has long been recognizedand several researchers have so far attempted to incorporate the flexibility of foundation in asymmetric system models [13-18]. Shakib and Fuladgar (2004) studied the dynamic soil-structure interaction effects on the seismic response of asymmetric buildings. An approach was formulated for them for the linear analysis of the three-dimensional dynamic soil-structure interaction of asymmetric buildings in the time domain. They found that the eccentricity ratio of asymmetric system has a significant effect on the response of soil-structure interaction system,which is strongly dependent upon the base flexibility and structural period of the system. In low structural period ($T_X = .5$), the displacements of symmetric buildings situated in very flexible and medium flexible soil conditions are considerably increased by increase of the eccentricity ratio. However, in the long structural period ($T_X = 2$) situated on the same soil conditions, the lateral displacements are decreasedand torsional displacementsare mildly increased by increase of the eccentricity ratio [19,20].Rana Roy and Sekhar Chandra (2010) studied the inelastic seismic demand of low-rise buildings with soil-flexibility by using two types of modeling; single story and real system. In all models, both elasto-plastic and degrading hysteresis behaviors for lateral load-resisting structural elements were considered, while sub-soil was idealized as linear and elasto-plastic in parallel. They concluded that inelastic response of the asymmetric structure relative to its symmetric counterpart is not appreciably influenced due to SSI. Their study also confirmed that equivalent single-story model, characterized by the lowest period rather than the fundamental one of the real system, tends to yield conservative estimation of inelastic demand at least for the short-period systems [21].

In all of the above studies, the behavior of asymmetric building was based on the traditional approach,i.e. it was assumed that stiffness and strength are independent in the LFREs of the buildings. In this study, an attempt was made to consider the effects of nonlinear dynamic soil–structure interaction on the behavior of asymmetric wall-type buildings. The behavior of asymmetric building was based on the new approach; the responses of the buildings for different distributions of mass, stiffness and strength were evaluated. Finding the desirable distribution in soil-structure system to reduce the torsional response so that the torsional effect becomes minimum was another purpose of this study. The asymmetric building used in this study was wall-type system and the SSI effect was modeled by 3D finite element method.

2. System Model and Formulation

A single-story idealized building resting on homogeneous soil surface was considered in this study (fig 1) The soil beneath the structure was divided into two

fields. In the near field, the bounded domain of the soil that can exhibit nonlinear behavior was considered. While, in the far field, the unbounded domain of the soil that extends to infinity was considered. As the amplitudes of stress decay with increasing of distance from the structure, the nonlinearity is limited to the bounded soil. The unbounded soil was assumed to behave linearly.
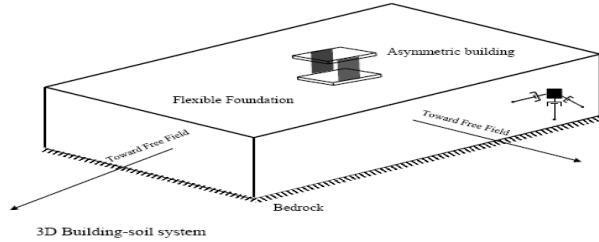

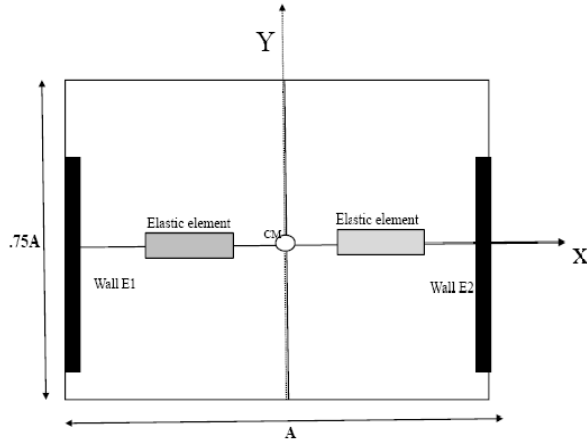**Fig. (1-a)** Soil-structure interaction system

Fig. (1-b) Asymmetric building plan

The soil bounded domain can be modeled by the standard finite-element method. In this domain, because of the inelastic properties of the soil, the nonlinear finite element was used and proper constitute model was assumed. In this paper, for modeling of the soil, Drucker-Prager constitutive model was used [22]:

$$f(J_2, I_1) = \sqrt{J_2} + \alpha I_1 - K \tag{1}$$

Where, I_1 and J_2 are the first and second invariants of the stress,respectively.This yield criterion is a pressure-dependent model for determining whether a material has failed or undergone plastic yielding and also to deal with the plastic deformation of pressure-dependent materials similar to the soil. To model the soil-structure interaction,a problem using the finite-element method is that the unbounded domain has to be truncated to a domain of finite size as the size of a finite element is finite.One of the common methods for assuming the effect of unbounded domain is replacing this domain with transmitting boundary conditions.Lysmer and Kuhlemeyer (1969)

proposed the first transmitting boundary that is often referred to as"classic viscous boundary condition". This boundary condition is formulated as follows:

$$\sigma = \rho V_p \dot{u} \tag{2-a}$$
$$\tau = \rho V_s \dot{v} \tag{2-b}$$

Where, σ and τ are the normal and shear stresses on the boundary, respectively,ρ is the mass density,and V_p and $V_s$are the longitudinal and shear wave velocities, respectively [12].

The superstructure of the system consists of a single rectangular uniform slab of plan dimensions Ax0.75A and weight W. Center of Mass located at the geometric centre of the slab. It is supported at the edges by two mass less elasto-plastic elements; Wall E-1 and Wall E-2, in the Y-direction. These elements may be identified as two reinforced concrete flexural walls having different lengths, and their yield displacements can be readily determined. The system is assumed to be mono-symmetric. The X-direction elasticelements are located along the axis of symmetry and do not contribute to any torsional resistance.

The yield displacements of WallE-1 and WallE-2 elements are taken to be δ and $\alpha\delta$, respectively. Where, α is the yield displacement distribution parameter,which was assumed to be equal to or greater than unity.In this study,α being greater than unity implies that the left edge wall has a larger length than the wall at the right edge.f and βf denote the nominal strengths of WallE-1 and WallE-2, respectively.Therefore, the total strength of the system is $(1 + \beta)f$. The location of CV is governed by the strength distribution parameter β. CV is located to the left of CM ifβ is less than unity, and to the right of CM when β is greater than unity. The stiffness of WallE-1 and WallE-2 is given by $k = \frac{f}{\delta}$ and γk, respectively. Where, $\gamma = \frac{\beta}{\alpha}$. The total lateral stiffness of the system is equal to $(1 + \gamma)k$. The CR location is governed by the stiffness distribution parameter,γ [8, 9].

The strength and stiffness eccentricity of this system can be evaluated according to the following relations:

$$e_V = \frac{\beta - 1}{\beta + 1} \times \frac{A}{2} \tag{3}$$
$$e_R = \frac{\gamma - 1}{\gamma + 1} \times \frac{A}{2} \tag{4}$$

If the distance from CR to CVis denoted by D, then:

$$D = e_V - e_R = \frac{\beta(\alpha - 1)}{(1 + \beta)(\alpha + \beta)}A \tag{5}$$

In which, D depends on the yield displacement distribution as well as on the strength distribution. The $\frac{D}{A}$ dependency onβ andα is shown in Figure (2). Within a wide range of strength distribution, $.5 \leq \beta \leq 2.0$, $D$is insensitive to the strength distribution parameter, β.

Using a fixed value of αequal to 1.4, five models were created, with βequal to 1.4, 1.2, 1.1, 1.0 and 0.8. They will

be referred to as models 1, 2, 3, 4 and 5, respectively. Both elements (Wall E-1, Wall E-2) in model 1 have the same stiffness, because $\gamma = \frac{\beta}{\alpha}$ is equal to 1. With reference to CM as the origin, it has zero stiffness eccentricity and positive strength eccentricity. In models 2 and 3, $\gamma < 1$ and $\beta > 1$, consequently CR is located on the left while CV is on the right of CM (balance condition). These models have negative e_R, but positive e_V. In model 4, $\beta = 1$ and $\gamma < 1$, therefore, it has zero strength eccentricity and negative stiffness eccentricity. Finally, model 5 represents the situation when both the stiffness and strength eccentricities have the same (negative) sign. Details of the strength and stiffness eccentricity of the mentioned models relative to CM are given in Table 1.

The described five models are resting on homogeneous soil surface, as shown in Figure 1. The walls of these models at the base are connected to a rigid mat foundation. In global co-ordinate system, the nonlinear 3-dimensional differential equation of the motion of soil–structure interaction system can be written as below [19]:

$$[M]\{\ddot{U}\} + ([C] + [C_{V1}] + [C_{V2}] + [C_{V3}] + [C_{V4}])\{\dot{U}\} + \{P(U)\} = F(t) \tag{6}$$
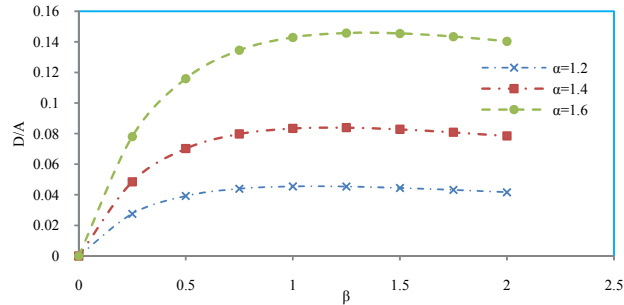
Where,

$$F(t) = -[M][R_g]\{\ddot{U}_g\} \tag{7}$$

Fig. (2) Variation of D/A relative to β

Table 1 Details of the strength and stiffness eccentricity of the five structural models

Models	α	β	strength eccentricity	stiffness eccentricity
1	1.4	1.4	right	zero
2	1.4	1.2	left	right
3	1.4	1.1	left	right
4	1.4	1	zero	left
5	1.4	0.8	left	left

Also {U} is the vector of displacement in global co-ordinate system relative to the bedrock, {$\dot{U}$} and {$\ddot{U}$} are the vectors of velocity and acceleration in global co-ordinate system relative to the bedrock, respectively, and [M] and [C] are the mass and damping of the whole system, respectively. In this study, Rayleigh damping was

used to construct the damping matrix $[C]$. $[C_{V1}]$ to $[C_{V4}]$ are the viscous boundary matrices on the four sides of the free field elements, $\{\ddot{U}_g\}$ is the earthquake ground acceleration vector at the bedrock and $\{R_g\}$ is the matrix of the influence of ground motions. $P\{(U)\}$ is system history dependent internal (inelastic) resisting force vector, which is a function of displacement. This vector is derived by assembling the elements internal (inelastic) resisting force vector.

The nonlinear equation of motion was solved numerically using the Newmark-β method, where it was assumed that $\alpha = o.5$ and $\beta = .25$[22, 23]. By applying this method into the Equation (6) and expressing it at discrete time $t = t_{n+1} = (n+1)\Delta t$, in which Δt denotes the constant time increment that yields the nonlinear equation in the unknown's $u_{n+1} = u(t_{n+1})$ the residual $\Psi(u_{n+1})$ is as follow:

$$\Psi(u_{n+1}) = \tilde{F}_{n+1} - \left[\frac{1}{\beta(\Delta t)^2}Mu_{n+1} + \frac{\alpha}{\beta(\Delta t)}Cu_{n+1} + P(u_{n+1})\right] = 0 \tag{8}$$

Where,

$$\tilde{F}_{n+1} = F_{n+1} - M\left[\frac{1}{\beta(\Delta t)^2}Mu_n + \frac{\alpha}{\beta(\Delta t)}C\dot{u}_n - \left(1 - \frac{1}{2\beta}\right)\ddot{u}_n\right] + C\left[\frac{\alpha}{\beta(\Delta t)}u_n - \left(1 - \frac{\alpha}{\beta}\right)\dot{u}_n - (\Delta t)\left(1 - \frac{\alpha}{2\beta}\right)\ddot{u}_n\right] \tag{9}$$

Assume that a Newton-Raphson iterative procedure is used to solve Equation (8) over the time step $[t_n, t_{n+1}]$. By solving a sequence of liberalized problems of the form:

$$\left(K_T^{dyn}\right)_{n+1}^i \delta u_n^{i+1} = \Psi_{n+1}^i \quad i = 0,1,2,\dots \tag{10}$$

Where,

$$\left(K_T^{dyn}\right)_{n+1}^i = \left[\frac{1}{\beta(\Delta t)^2}M + \frac{\alpha}{\beta(\Delta t)}C + (K_T^{stat})_{n+1}^i\right] \tag{11}$$

and

$$\Psi^i(u_{n+1}) = \tilde{F}_{n+1} - \left[\frac{1}{\beta(\Delta t)^2}Mu^i_{n+1} + \frac{\alpha}{\beta(\Delta t)}C^iu_{n+1} + P(u^i_{n+1})\right] \tag{12}$$

The updated nodal displacement vector u_{n+1}^{i+1} or displacement vector at the end of the iteration #$(i+1)$ of time step $[t_n, t_{n+1}]$ is obtained as:

$$u_{n+1}^{i+1} = u_n + \Delta u_n^{i+1} = u_{n+1}^i + \delta u_n^{i+1} \tag{13}$$

Where Δu_n^{i+1} and δu_n^{i+1} denote the total incremental displacement vector from the last converged step and the last incremental displacement vector, respectively. In Equation (11), $\left(K_T^{dyn}\right)_{n+1}^i$ denotes the tangent dynamic stiffness matrix. The consistence tangent stiffness matrix $(K_T^{stat})_{n+1}^i$ in Equation (11) is obtained as:

$$K_T^{stat} = \frac{\partial P}{\partial a} = \int_V B^T D^{ep} \, BdV \qquad (14)$$

In the aboveequation, D^{ep} is the elasto-plastic constitutive matrix. This matrix is related to Constitutive Models, which are used for system materials.

3. Numerical Study

To verify the effect of soil–structure interaction on the response of asymmetric buildings, an idealized three dimensional single-storeysoil-structure system was studied. To provide a target for comparison, a symmetric fixed structural model was created,which will be referred to as model R. It has identical elements at the edges and the stiffness of each element is adjusted such that this system has the same lateral period and similar lateral strength. Since, there will be no torsional response; the results obtained from this model represent translation response only. The reference structural model (i.e., R) consists of a single rectangular uniform slab of plan dimensions 12×9 m and weight W=1265 KN. One can design the model so as to have a lateral period of T =0.63sec and an overall nominal strength of 0.2W, i.e. 253 KN. The CM is located at the geometric centre of the slab. It is supported at the edges by the two mass less elasto-plastic elements of Wall-E1 and Wall-E2 in the Y-direction(Figure1.a). These elements may be identified as two reinforced concrete flexural walls having different lengths. The walls yield displacements can be readily determined [5].

The single-storey soil-structure system was assumed to be mono-symmetric. Such a model was used to illustrate torsional phenomena in ductile soil-structure systems. So one can focus on the mechanism of the inelastic response process and obtain a physical understanding of the behavior of asymmetrical soil-structural systems. Damping in the soil and structure has been modeled by Rayleigh method. The damping ratio of the soil and the structure is assumed to be equal to 7 and 5 percent of the critical damping, respectively.It is to be noted that the damping of the soil medium is a function of the shear strain.

The damping ratio of sand varies between about 2 percent for shear strain equal to 0.0001 to 16 percent for shear strain equal to 0.0008 [24].The details of the strength and stiffness of the six fixed models are shown in table2. It is worth mentioning that the same properties were assumed for the five asymmetric super-structures of the soil-structure models.

The soil beneath the structure was modeled with non-linear solid elements. The solid element has eight nodes with three degrees of freedom at each node. The far field boundary was modeled by using "dashpot". Height of the soil over the bedrock was assumed to be 30 m and the bounded soil was taken to be 150x90 m.

Table 2 Details of the strength and stiffness of the models

Models	strength(KN)		stiffness(KN/m)		yield displacements(m)	
	Wall-1	Wall-2	Wall-1	Wall-2	Wall-1	Wall-2
R	126	126	5412	5412	.0234	.0234
1	105	147	5412	5412	0.0195	0.0273
2	113	136	5828	4995	0.0195	0.0273
3	118	129	6061	4762	0.0195	0.0273
4	123	123	6315	4508	0.0195	0.0273
5	134	107	6889	3934	0.0195	0.0273

The maximum dimension of the mesh of solid elements was chosen in the following form:

$$\Delta l_{max} \leq \left(\frac{1}{10}\right)\lambda \qquad (15)$$

Where λ is the wavelength associated with the highest frequency component that contains appreciable energy. Maximum element size was selected to be 2 m which satisfies the condition state in Equation (15) [25]. The effects of slip as well as the separation of the foundation mat on the response behavior of asymmetric systems were not considered in the present paper; rather we assumed three types of soil (Table 3).

Table 3 Properties of the soil

soil	shear wave velocity	mass density	Poisson's ratio
TYPE	(m/sec)	(ton/m^3)	---
I	800	1.9	0.4
II	300	1.8	0.3
III	100	1.7	0.3

All models were excited along the Y-direction by a widely used earthquake ground motion: the NS component of the 1940 El Centro earthquake record, amplified by a factor of 1.5. In soil-structure system the earthquake was applied to the bedrock of models, while for the fixed cases, it was applied to the system base.

In order to verify the modeling process, the free vibration analysis was carried out both on the symmetric fixed base condition and on the symmetric soil-structure models situated on different soil conditions. The time periods of the first three modes of vibrations for different cases of the buildings are shown in Table 4. As shown, time periodsof the soil type-I are the same as in the fixed base condition. While the time periods of the symmetric system with the soil type-III are considerably increased compared to the period of the symmetric system with fixed base condition. Also, the period of the system with soil type-II shows similar pattern as its period with soil type-III. The nonlinear dynamic analyses were also carried out on the symmetric fixed base system as well as on the symmetric soil-structure model with different soil conditions for the verification purposes. The variations of normalized nonlinear displacement on the time history of the systems subjected to El Centro earthquake component are shown in figure. 3. As expected, the normalized

nonlinear displacement time history of the system with fixed base condition and the symmetric soil-structure system with the soil type I (i.e. Vs=800m/sec) is almost the same. However, as it shown in figure.3,the normalized nonlinear displacement is increased for the symmetric soil-structure systems with softer soils.

Table 4 Eigen value analysis of symmetric systems

Mode	Period (sec)			
	Fix	Type(I)	Type(II)	Type(III)
Y-Direction	0.63	0.63	0.76	1.23
X-Direction	0.24	0.25	0.41	0.72
Rotation	0.13	0.13	0.3	0.58
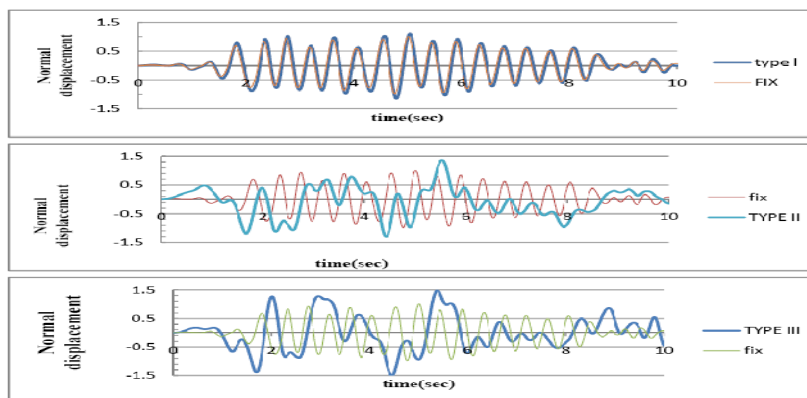
Fig. 3 Variation of normalizeddisplacement response time history of the symmetric buildings on three soil conditions

3.1. Response of the models

Statistics of the various parameters of interest are summarized in Tables 5 to 8. Table 5 is for fix case system and Tables 6-8 are for the soil-structure systems with three different soils types. In all tables, the peak displacements at the edges are shown in the columns 2 and 3. For model R (symmetric model), the base flexibility decreases the ductility and peak displacements. To explain this trend, it should be noted that base flexibility has subtractive effect on base shear, so the lateral displacement decreases. The response quantities in Table 5 and Table 6 are approximately same.

It means that the response of fixed case models is similar to the soil-structure models with the soil type I.As Tables 7-8 show, the soil-structure interaction has subtractive effect on the responses. In four cases, out of the five asymmetric models, model 1 has the largest left edge displacement while model 5 has the largest right edge displacement. For model 1, in absolute terms, the left edge displacement for cases 1,2,3, and 4 is0.228, 0.221,0.184,and 0.115, respectively. For model 5,in absolute terms, right edge displacement for cases 1,2,3and 4 is0.241, 0.237,0.198, and 0.118, respectively. This shows that,as the base flexibility increased the scattering of the left and right edges displacementis reduced. To explain this scattering, it is important to note that,in each case,the base flexibility decreases the soft edge displacement more than the stiff edge.

Table 5 Peak responses for the set of models in the case (1)(fix)

model	Peak displacement(m)				Peak ductility		Peak
	Edge	Edge	CM	CM			rotation
	left	right	Ave	Resp	E1	E2	01 (rad)
R	0.168	0.168	0.168	0.168	7.2	7.2	0.00
1	0.228	0.132	0.180	0.172	11.7	4.8	0.70
2	0.201	0.165	0.173	0.174	10.3	6.0	0.19
3	0.181	0.185	0.173	0.174	9.3	6.8	0.10
4	0.158	0.205	0.181	0.173	8.1	7.5	0.43
5	0.116	0.241	0.179	0.165	5.9	8.8	1.12

Table 6 Peak responses for the set of models in the case (2) (structure and soil type –I)

model	Peak Displacement(m)				Peak ductility		Peak
	Edge left	Edge right	CM Ave	CM Resp	E1	E2	rotation .01 (rad)
R	0.164	0.164	0.164	0.164	7.01	7.01	0.0080
1	0.221	0.130	0.175	0.172	11.33	4.76	0.68
2	0.195	0.163	0.175	0.174	10.00	5.97	0.19
3	0.178	0.180	0.175	0.174	9.13	6.59	0.10
4	0.155	0.197	0.176	0.172	7.95	7.22	0.39
5	0.115	0.237	0.176	0.168	5.90	8.68	1.08

Table 7 Peak responses for the set of models in the case (3) (structure and soil type-II)

model	Peak Displacement(m)				Peak ductility		Peak
	Edge left	Edge right	CM Ave	CM Resp	E1	E2	rotation 01 (rad)
R	0.144	0.144	0.144	0.143	6.14	6.14	0.001
1	0.184	0.109	0.147	0.149	9.45	3.99	0.46
2	0.159	0.134	0.147	0.146	8.17	4.91	0.13
3	0.141	0.152	0.146	0.146	7.23	5.55	0.06
4	0.132	0.160	0.146	0.148	6.76	5.84	0.29
5	0.094	0.198	0.146	0.143	3.62	6.88	0.74

Table 8 Peak responses for the set of models in the case (4)(structure and soil type-III)

model	Peak Displacement(m)				Peak ductility		Peak
	Edge left	Edge right	CM Ave	CM Resp	E1	E2	rotation 01 (rad)
R	0.115	0.115	0.115	0.115	4.91	4.91	0.005
1	0.115	0.068	0.092	0.093	5.92	2.49	0.320
2	0.096	0.082	0.089	0.089	4.93	2.98	0.080
3	0.082	0.096	0.089	0.089	3.99	3.63	0.040
4	0.078	0.099	0.088	0.091	3.26	4.03	0.200
5	0.059	0.118	0.093	0.082	3.03	4.80	0.530

According to the data shown in the above tables, it can be concluded that the model with the largest edge displacement does not necessarily have the largest ductility demand on its elements. The peak ductility demands for each element are shown in the columns6 and 7 of the above tables. Model 1 has the largest ductility demand at the left edge while model 5 has the largest ductility demandat the right edge. The effect of SSI on ductility demands is subtractive so that maximum of the ductility demands in model 1for the cases 1, 2, 3, and 4 is 11.7,11.33,9.45and 5.92, respectively. To explain why model 5 has the largest edge displacement while model 1 has the largest ductility demand, one should note that the element yield displacements are not the same. The right element of the models has1.4 times larger yield displacement than that of the left element.The soil-structure models also revealed the necessity to examine both the displacement and ductility responses in any seismic response study of asymmetric systems. As pointed out by W.K.Tso, strength distribution designed to minimize ductility in the base flexible structures may not lead to minimum displacement as the fixed base structures [8, 9]. In all cases,the results of models 2 and 4 showed more balanced responses for both the edge displacements and the element ductility demands.

Slab rotation is another response parameter, which is extensively used to study the behavior of asymmetric buildings. In all cases, model 3 has the smallest slab rotation, as shown in the column 8 of the above tables. Like edge displacement and ductility, SSI has subtractive effect on slab rotation so that this response for model 3in four cases is0.001, 0 .001, 0.0006and 0.0004, respectively. In model 3, CR and CVare situated on the opposite sides of CM. This is a condition referred to as 'balanced CV–CR

location' for soil-structure system. In this condition, a desirable distribution of mass, stiffness and strength to reduce torsional response is attained. The same conclusion has also been derived by Tso and Myslima (2002, 2005) for fixed condition[8, 9].

The peak CM displacement obtained using the procedure given by W.K.Tsois presented in the column 4 of Tables5-8 and named as the estimate CM displacement [8, 9]. The peak response displacement at the CM, as determined using dynamic analysis, is presented in the column 5 of the tables. A comparison between columns 4 and 5 shows the accuracy of the CM displacement estimate. The CM displacement estimate is exact if the peak edge displacements are reached at the same instant of time. Otherwise, the estimate is always larger than the true peak of CM displacement. For the four cases considered in model 3, the estimate and determined CM displacement are equal, but in the other models, these two values are not

equal. For example, in model 5, the overestimation goes up to 10%.

While a comparison of peak responses generally provides a useful summary, an examination of the time histories leads to a better understanding of the model's behavior. The element displacement time histories are presented in Figures4-7. In model 1, the left edge(L) has a larger displacement than the right edge(R) and the reverse is true for models4 and 5. The response trace of model 3 shows that displacement traces of both edges in this model are similar while in model 5, this response has the minimum similarity. In all cases, SSI effect changes the numerical value of displacements and shows the same pattern of variation compared to the fixed case. For all models, the base flexibility of models causes the similarity of two edges displacement to increase so that, for soft soil in all models, displacement of these two edges is approximately similar.
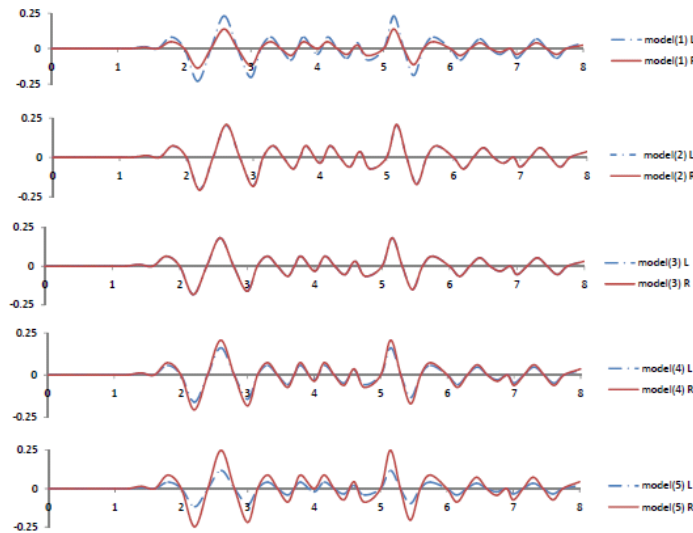

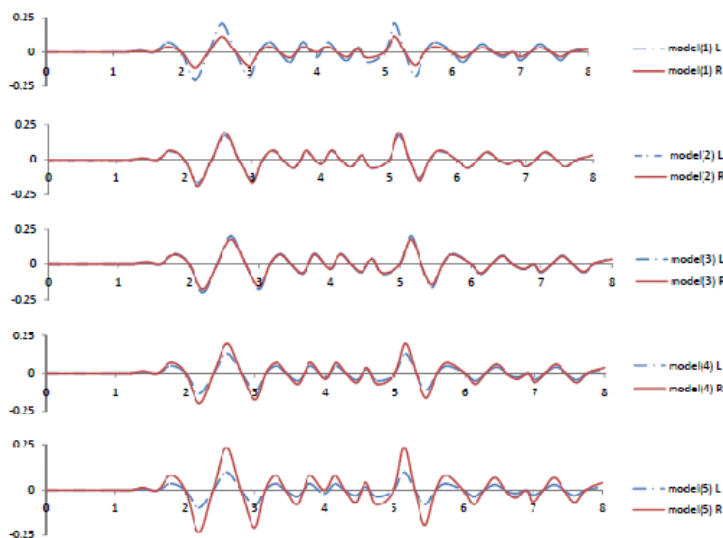**Fig. 4** Time history of displacement forthe case (1) (fix)

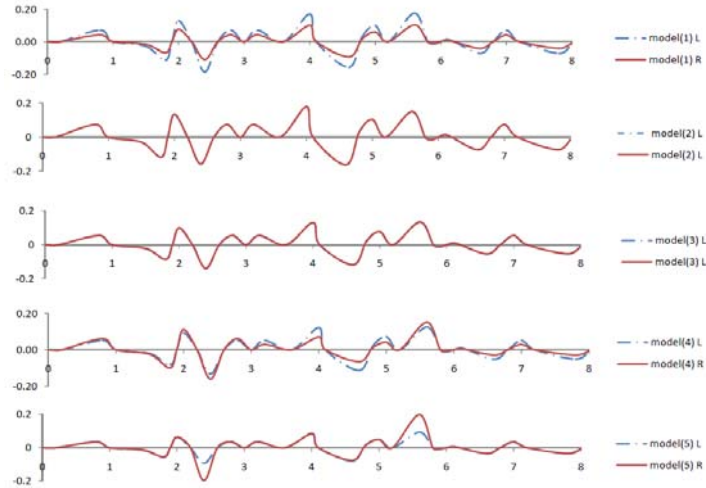**Fig. 5** Time history of displacement for the case (2) (soil type-Iand structure)

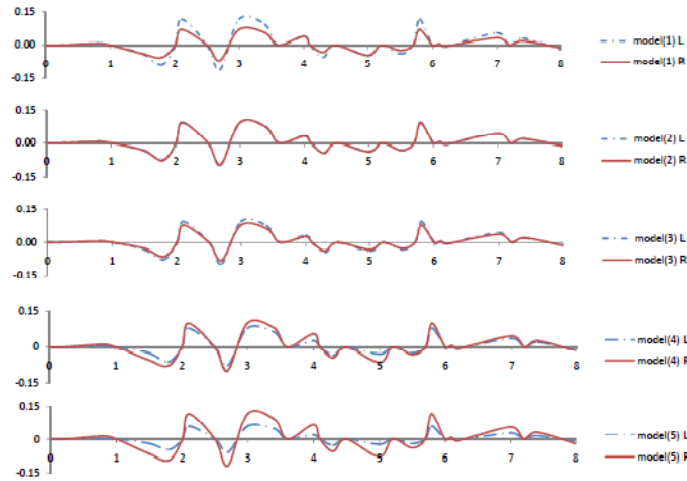**Fig. 6** Time history of displacement for the case (3) (soil type-IIand structure)

Fig. 7 Time history of displacement for the case (4) (soil type-IIIand structure)

4. Rotational Responses

A clearer picture on how torsion affects the behavior of the soil-structure models can be obtained by focusing on their rotational responses. One can state that the lower is the rotational response; the less susceptible is the system to torsional damage. The maximum rotation experienced by the slab in each model is included in Tables 4-6. Fig.8 shows a clear understanding of the slab rotation. As shown, model 5 shows the highest rotational response, while model 3 shows the least slab rotation. It is interesting to note that as the soil becomes softer, the slab rotation reduces considerably. The soil-structure interaction modifies the torsional responses. Figure 8 also shows that the effect of foundation flexibility is decretive.

The slab rotation time histories of these models are shown in Figures 12-15. An examination of the slab rotation traces reveals that model 5 has the largest rotation.

The rotation magnitudes in models 1 and 4 seem to be almost similar. Model 1 tends to have a negative rotation, enhancing the left edge displacement and making the displacement at the left edge of the critical response parameter. Model 4 tends to have a positive rotation, promoting the right edge displacement. Finally, models 2 and 3 have the smallest rotations and both of them tend to oscillate about the mean equilibrium position. The pattern of response variation is almost the same in the fixed case, and the SSI effect changes only the numerical value of the time history responses. For soft soil condition, the slab rotation is minimum comparing to the other cases, and model 3 has the minimum rotation relative to the other models.
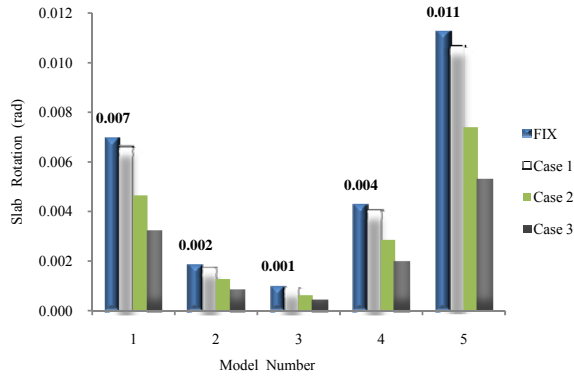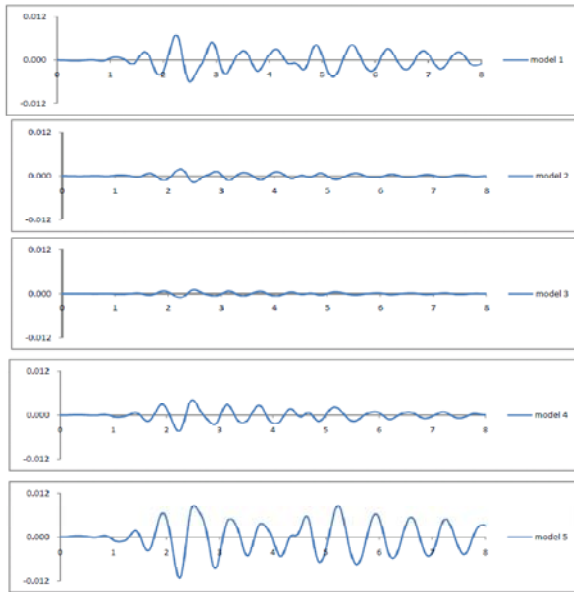
Fig. 8 Peak of slab rotation for five models

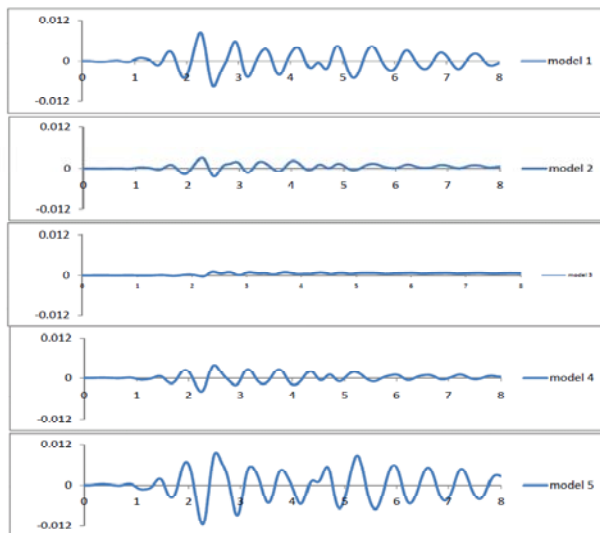**Fig. 9** Rotation time histories of slab in the case (1) (fix)

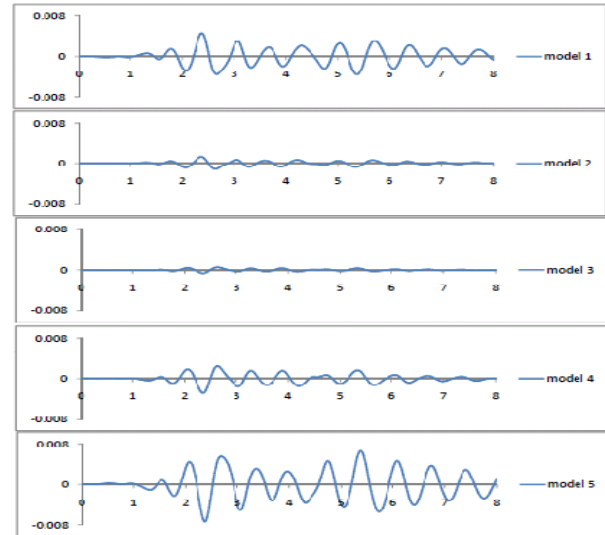**Fig. 10** Rotation time histories of slab in the case (2) (soil type I and structure)

Fig. 11 Rotation time histories of slab in the case (3) (soil type II and structure)
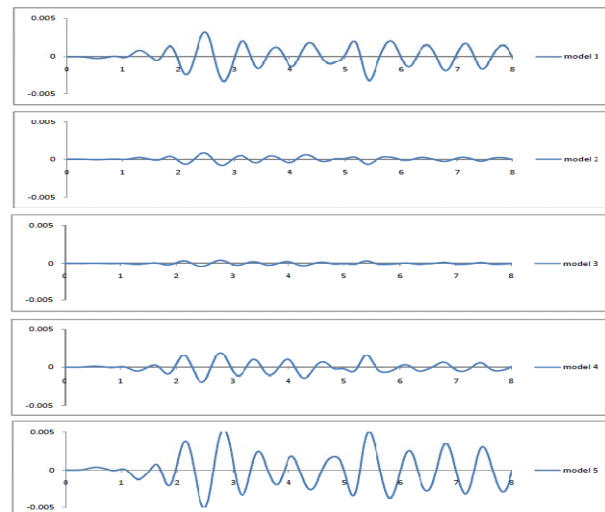

Fig. 12 Rotation time histories of slab in the case (4) (soil type III and structure)

5. Conclusion

Three-dimensional soil–structure interaction behavior of asymmetric wall-type system subjected to NS component of El Centro 1940 earthquake records and for different positions of stiffness and strength eccentricity was investigated. The study findings led to the following conclusions:

1.   Large ductility demand occurred in zero stiffness condition but peak displacement demand occurred in the case that CV and CR were in one side of CM. In two cases, SSI effect decreased these demands so that in soft soil condition, these demands were approximately 50% of fixed condition.

2.   As the base flexibility increased, the scattering of the stiff and soft edges displacement was reduced.

3. Minimum torsional response occurred when CV and CR were in the opposite sides of CM (balance condition) and SSI had no effect on this criterion.

4. In all cases, foundation flexibility decreased the torsional response of the building so that the soft soil had the maximum effectand, for very stiff soils, this effect was negligible. For example, in the balance condition, the difference between rotational demand for soft soil and fixed base condition was 60%.

5. In the fixed case and the structure with flexible base, unlike the traditional approach, the zero stiffness eccentricity not only led to minimum torsional responsebut also itcaused the increase ofthis response.

In different patterns of strength and stiffness distribution, the worst case was the one where stiffness and strength center(CR and CV)were on one side of CM, and base flexibility didnot change this criterion.

References

[1] Hejal R, Chopra AK. Earthquake analysis of a class of torsionally coupled buildings, Earthquake Engineering and Structural Dynamics, 1989, No. 3, Vol. 8, pp. 305–323.

[2] Kan CL, Chopra AK. Elastic earthquake analysis of torsionally coupled multi-story buildings, Earthquake Engineering and Structural Dynamics, 1977, No. 2, Vol. 5, pp. 395–412.

[3] Kan CL, Chopra AK. Simple model for earthquake response studies of torsionally coupled buildings, ASCE Engineering Mechanic Division, 1981, No. 4, Vol. 6, pp. 235–251.

[4] Tasnimi A, Rezazadeh M. Experimental and numerical analysis of strengthened single storey brick building under torsional moment, IJCE, 2012, No. 3, Vol. 10, pp. 7-7.

[5] Priestley MJN, Kowalsky MJ. Aspects of drift and ductility capacity of rectangular cantilever structural walls, Bulletin of the New Zealand Society for Earthquake Engineering, 1998, No. 5, Vol. 10, pp. 73–85.

[6] Tso WK, Myslimaj B. A yield displacement distribution-based approach for strength assignment to lateral force-resisting elements having strength dependent stiffness, Earthquake Engineering and Structural Dynamics, 2003, No. 2, Vol. 10, pp. 2319–2351.

[7] Myslimaj B, Tso WK. A design-oriented approach to strength distribution in single story asymmetric systems with elements having strength-dependent stiffness, Earthquake Spectra, 2005, No. 2, Vol. 21, pp. 197–212.

[8] Myslimaj B, Tso WK. A strength distribution criterion for minimizing torsional response of asymmetric wall-type systems, Earthquake Engineering and Structural Dynamics, 2002, No. 2, Vol. 31, pp. 99 –120.

[9] Aziminejad A, Moghadam AS. Performance of asymmetric multi story shears buildings with different strength distributions, Journal of applied sciences, 2009, No. 6, Vol. 9, pp. 1082-1089.

[10] Shakib H, Ghasemi A. Considering different criteria for minimizing torsional response of asymmetric structures under near-fault and far-fault excitations, International Journal of Civil Engineering, 2007, No. 4, Vol. 5, pp. 247-265.

[11] Aziminejad A, Moghadam AS. Fragility-based performance evaluation of asymmetric single-story buildings in near field and far field earthquakes, Journal of Earthquake Engineering, 2010, No. 6, Vol. 14, pp. 789-816.

[12] Ghanbari A, Hoomaan E, Mojallal M. An analytycal method for calculating the natural frequency of retaining walls, IJCE, 2013, No. 1, Vol. 11, pp. 1-9.

[13] Balendra T, Tat CW, Lee SL. Modal damping for torsionally coupled buildings on elastic foundation, Earthquake Engineering and Structural Dynamics, 1982, No. 2, Vol. 10, pp. 735–756.

[14] Tsicnias TG, Huchinson GL. Soil–structure interaction effects on the steady state response for torsionally coupled buildings with foundation interaction, Earthquake Engineering and Structural Dynamics, 1984, No. 2, Vol. 12, pp. 237–262.

[15] Chandler AM, Hutchinson GL. Code design provisions for torsionally coupled buildings on elastic foundation, Earthquake Engineering and Structural Dynamics, 1987, No. 2, Vol. 15, pp. 517–536.

[16] Sivakumumaran KS, Lin MS, Karasudhi P. Seismic analysis of asymmetric building-foundation systems, Computers and Structures, 1992, No. 3, Vol. 43, pp. 1091–103.

[17] Sivakumuaran KS, Balendra T. Seismic analysis of asymmetric multi storey buildings including foundation interaction and P effects, Engineering Structures, 1994, No. 2, Vol. 16, pp. 609–625.

[18] Wu WH, Wang JF, Lin CC. Systematic assessment of irregular building-soil interaction using efficient modal analysis, Earthquake Engineering and Structural Dynamics, 2001, No. 2, Vol. 30, pp. 573–594.

[19] Shakib H, Fuladgar A. Dynamic soil–structure interaction effects on the seismic response of asymmetric buildings, Journal of StructuralEngineering, 2003, No. 5, Vol. 5, pp. 1841–1850.

[20] Shakib H. Evaluation of dynamic eccentricity by considering soil–structure interaction: a proposal for seismic design codes, Soil Dynamics and Earthquake Engineering, 2004, No. 2, Vol. 24, pp. 369–378.

[21] Rana Roy, Sekhar Chandra Dutta. Inelastic seismic demand of low-rise buildings with soil-flexibility, International Journal of Non-Linear Mechanics, 2010, No. 4, Vol. 45, pp. 419-432.

[22] Zienkiewicz OC, Taylor RL. The finite element method: 2. Physics Series, McGraw-Hill International Editions, 1998.

[23] Chopra AK. Dynamics of structures: theory and applications to earthquake engineering, Englewood Cliffs, NJ: Prentice-Hall, 1995.

[24] Choi J.S, Kim J.M. Earthquake response analysis of the hualien soil structure interaction system based on updated soil properties using forced vibration test data, Earthquake Engineering and Structural Dynamics, 2001, No. 3, Vol. 30, pp. 1-26.

[25] Bagherzadeh A, Ferdowsi B. Dynamic analysis of esfahan metro tunnels, Journal of Applied Sciences, 2009, Vol. 9, pp. 671-679.